Bioresource Technology Reports 34 (2026) 102840

Contents lists available at ScienceDirect

Bioresource Technology Reports

journal homepage: www.sciencedirect.com/journal/bioresource-technology-reports

Integral cassava valorization: Evaluation of derivatives to produce functional and sustainable materials

Nayara Balaba [a,b,*], Julia de Oliveira Primo [a,b], Xavier Noirfalise [a], Luiz Felipe Bodnar [c], Rafael Emil Klumpp [d], Carla Bittencourt [a], Fauze Jaco Anaissi [b]

[a] *Chimie des Interactions Plasma-Surface (ChIPS), Research Institute in Materials Science and Engineering, Université de Mons, Av. Nicolas Copernic 3, 7000, Mons, Belgium*

[b] *Chemistry Department, University Estadual do Centro-Oeste, UNICENTRO, Alameda Elio Antonio Dalla Vecchia, 838, 85040-167, Guarapuava, PR, Brazil*

[c] *Food Engineering Department, University Estadual do Centro-Oeste, Guarapuava, 85040-080, Brazil*

[d] *Materials Science Department, Faculty of Engineering, University of Mons, 20, Place du Parc, Mons, 7000, Belgium*

A R T I C L E I N F O

Keywords:
Cassava
Agro-industrial by-products
Biomass valorization
Sustainable materials
Green synthesis
Circular economy

A B S T R A C T

Cassava (*Manihot esculenta* Crantz) is a staple crop of high socioeconomic relevance, and its industrial processing generates large volumes of by-products with potential for valorization. In this study, cassava cultivated in southern Brazil (Palmital, Paraná) was processed, and the derivatives: starch, fiber, and cassava wastewater (manipueira) were systematically separated and characterized to assess their complementary potential for sustainable material development. The starch showed a type A semi-crystalline structure (XRD) with granules averaging 10.8 μm, low acidity (1.58%), and low ash content (0.13%). Thermogravimetric analysis indicated near-complete decomposition below 380 °C, supporting its use as a clean organic fuel, polymeric matrix, and precursor for biodegradable films. XPS revealed high surface oxygen content (40%), indicating suitability for combustion synthesis. The fibers exhibited a lignocellulosic composition with a rough, fibrillar morphology (SEM), higher mineral content, moderate acidity (2.30%), and multistage thermal degradation, suggesting greater thermal stability and potential applications in activated carbon, composites, and catalytic supports. The manipueira was an amorphous aqueous derivative (99.7% moisture), rich in organic and inorganic compounds, with near-neutral pH (6.54) and major thermal decomposition at 605 °C with 66% mass loss, indicating its potential as a liquid precursor, dispersing medium, or reducing agent in combustion-assisted and sol–gel routes. Overall, the derivatives displayed distinct yet complementary properties, enabling the full valorization of cassava biomass and its processing streams, minimizing waste generation, supporting the development of functional materials through sustainable, low-impact pathways, and reinforcing cassava as a strategic feedstock for circular agro-industrial systems.

1. Introduction

Cassava (*Manihot esculenta Crantz*) is a shrubby, perennial plant in the family Euphorbiaceae, native to South America, and is propagated vegetatively by stem cuttings. In Brazil, it is one of the most traditional and popular foods, known as aipim, macaxeira, or cassava, depending on the region (Veiga et al., 2016). It is an important raw material for traditional communities, such as those in the Amazon region of Brazil, because of its socio-economic links to family farming, food security, and the practicality and simplicity of production, even under adverse conditions (Menezes et al., 2019).

There are several varieties of cassava known worldwide, and, depending on their purpose, they can be classified as bitter or sweet cassava based on their hydrocyanic acid (HCN) content (de Queiroz et al., 2020). Cyanogenic glycosides are present in different types of cassava and can vary with plant variety, age, soil, and climate (Maciel et al., 2023). For industrial use, cassava with a higher HCN concentration, known as ‘bitter cassava’, is preferred for its higher productivity and hardiness˙(Menezes et al., 2019). However, this type of cassava has a high linamarin content, which, if not processed correctly, can pose health risks and contaminate the environment by releasing free cyanide (CN-) and/or HCN (de Queiroz et al., 2020; Maciel et al., 2023). The

* Correspondent author.
E-mail address: nayara.balaba@student.umons.ac.be (N. Balaba).

https://doi.org/10.1016/j.biteb.2026.102840
Received 18 March 2026; Received in revised form 4 May 2026; Accepted 23 May 2026
Available online 25 May 2026

processing results in washing the starch and fiber, producing a large quantity of a yellow broth, the cassava wastewater (manipueira) in the industry, a residue rich in sugars, starches, proteins, linamarin, lotaustralin, salts, and cyanogenic derivatives (hydrocyanic acid, cyanides, and aldehydes) (Rebouças et al., 2015).

Cassava can be processed to obtain starch, a by-product that can be extracted by decantation and centrifugation. This product, also known as gum or sweet starch, can be produced either artisanally or industrially, differing only in the equipment used. Other products can be made from starch, such as sour flour, tapioca, sagu, beiju flour, and biscuits (Ferreira Filho et al., 2013; Rebouças et al., 2015). Starch is a biodegradable polysaccharide that stores the highest energy reserves in plants, occurring in stems, seeds, roots, and tubers. Among all polysaccharides, starch is the only one that forms small aggregates of linear or ramified structures that can be compacted into a birefringent semicrystalline complex called granules, which vary in size and shape from plant to plant (Brito et al., 2011). The two polymeric structures that make up starch are amylose and amylopectin, both formed by α-D-glucopyranose monomers capable of binding through α-d-(1,4) and α-d-(1,6) glycosidic bonds, thus forming starch granules (Brito et al., 2011; Jorge et al., 2023).

Cassava pulp is also generated in large quantities, approximately 10% of the raw material, and contains 40%–60% starch bound in residual fibers (Khejornsart et al., 2022; Prasertsilp et al., 2023). This by-product has been widely used for economic and environmental applications, including food, animal feed, compost, organic fertilizer, and biogas production (Watcharamongkol et al., 2024). The fibers of cassava consist of lignocellulose, mainly composed of lignin and hemicellulose (holocellulose). Cassava fibers of cassava consist of lignocellulose, mainly lignin, hemicellulose (holocellulose), and cellulose (Neto et al., 2015). Lignin is a complex polymer that forms the cell wall of plant fibers and imparts rigidity to plants (Brito et al., 2011; Neto et al., 2015). Cellulose, the main polymer in the fiber, is composed of glucose units linked by β1–4 glycosidic bonds, which are rigid and highly resistant to hydrolysis and contain certain crystalline regions (Neto et al., 2015). Unlike cellulose, hemicellulose is not chemically homogeneous, has a low molar mass, and lacks crystalline regions, making it more susceptible to hydrolysis under milder conditions. Its structure and composition vary depending on the natural source (Ogata, 2013). It is composed of pentoses, hexoses, and/or uronic acids (Silva Neto et al., 2015). Fig. 1 shows the main chemical structures present in starch (a), fiber (b), and manipueira (c).

Given the structural and functional diversity of cassava-derived components and their high potential as renewable biomass, this study aims to isolate, characterize, and analyze in depth cassava starch, fibers, and manipueira. The main objective is to examine their physicochemical, morphological, and structural properties to evaluate their potential as organic precursors for novel materials. By utilizing advanced characterization methods, this research seeks to establish clear links between the composition, structure, and reactivity of these cassava-derived materials. Such insights will help identify modification pathways and functionalization strategies, enabling their use as additives, polymer matrices, structuring agents, or modifiers in hybrid material synthesis systems (de Oliveira Schmidt et al., 2023; Pei et al., 2024; Travalini et al., 2019).

Recent advancements in biomass valorization, green synthesis, and functional material development have significantly expanded the scope of sustainable material research. Studies such as those by (Dugganaboyana et al., 2025; Guan et al., 2025; Guo et al., 2024; Jayaraman et al., 2026; Jiang et al., 2025; Kannappan et al., 2025; Kumarasamy et al., 2024; Natarajan et al., 2025; Pei et al., 2024; Pei et al., 2026; Ponnusamy et al., 2026; Prabhakaran et al., 2025; Sugumar et al., 2025) have explored innovative approaches to utilizing biomass-derived resources for the synthesis of eco-friendly materials, emphasizing the importance of reducing environmental impact while enhancing material functionality. These works collectively highlight the potential of green synthesis techniques in producing advanced materials for applications ranging from biomedicine to food science and nanotechnology. The methodologies and findings presented in these studies align with the broader goals of this research, which focuses on leveraging cassava starch-based systems and biomass-derived components to develop functional materials. By situating the present work within these recent developments, this study contributes to the growing body of knowledge aimed at achieving sustainable solutions in materials science.

Although previous studies have explored the properties and applications of individual cassava-derived fractions such as starch, fiber, or manipueira, these investigations are typically conducted in isolation and do not address the full valorization potential of the biomass. In this context, the present study proposes an integrated approach to simultaneously isolate and characterize starch, fiber, and manipueira from the same processing route. This strategy enables a consistent and

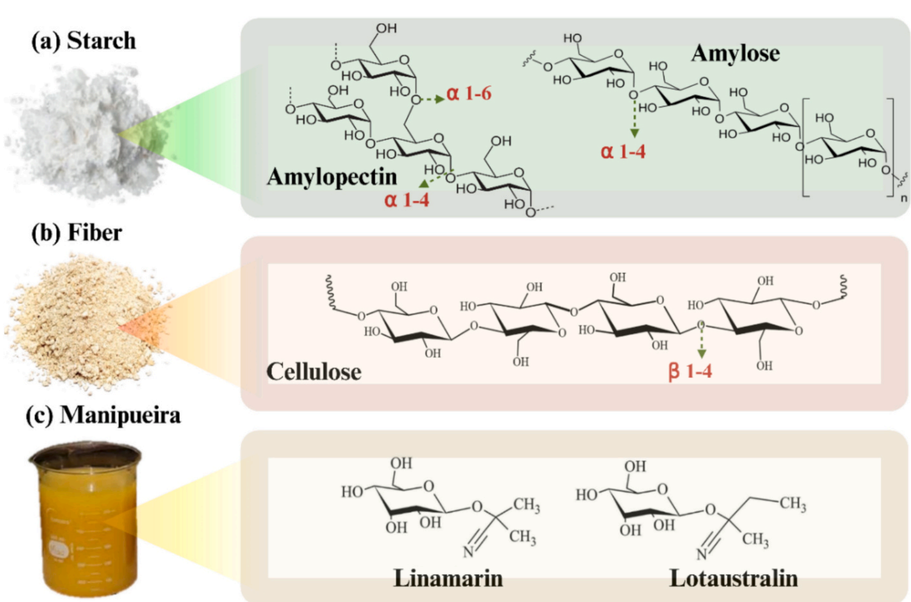

Fig. 1. Main structures present in (a) starch (amylose amylopectin); (b) fiber (cellulose), and (c) manipueira (linamarin and lotaustralin).

comparative evaluation of their physicochemical, structural, and thermal properties. Furthermore, this work goes beyond conventional characterization by linking these properties to their functional roles as organic precursors in the synthesis of sustainable materials. By demonstrating the complementary behavior of these derivatives within a unified framework, this study contributes to the development of circular strategies for agro-industrial residues. It advances the concept of complete biomass valorization toward low-impact material production.

2. Materials and methodology

The starch, fiber, and cassava wastewater (manipueira) used were obtained from the same yellow- and white-pulp cassava cultivars (both varieties of the botanical species *Manihot esculenta Crantz*), harvested in the Palmital region of Paraná, Brazil (24° 54′ 55.864″S (latitude) and 52° 17′40.263″ W (longitude)). Notably, both yellow- and white-pulp cassava cultivars were grown and processed together in this study. This approach was intentionally adopted to reflect typical agro-industrial practices, in which different cassava varieties are often combined during processing. Although it is well established that cassava cultivars may exhibit significant variations in starch content and structural composition (Li et al., 2026), the resulting derivatives in this work represent an averaged composition, suitable for evaluating general structure–property relationships and their potential application in material synthesis, rather than cultivar-specific differences.

In this work, cassava waste valorization refers specifically to residues generated during the conventional wet processing route for cassava starch extraction (the main product from cassava). This process consists of the mechanical crushing of cassava roots with water, followed by the separation of the fibrous derivative and the sedimentation of starch. As a result, three main derivatives are obtained: starch (sedimented solid), fiber (insoluble residue), and manipueira (liquid supernatant), which is the primary wastewater of this process. The steps involved in extracting and preparing the extract are described below:

Step 1 – Cassava cleaning and processing: The initial step involves thoroughly washing the cassava roots under water to remove residual impurities and unwanted organic matter, such as soil and plant debris. Subsequently, the outer brown peels are carefully removed with a food-grade sponge, leaving only the white inner peel and the tuber pulp. For processing (Fig. 2), the cleaned roots are mechanically crushed in an industrial blender (Industrial Blender Spolu Attak 1.75 L High Speed Stainless Steel, 220V). A cassava-to-water ratio of 1:3 (m/m) is used to facilitate efficient processing and fiber breakdown, resulting in a thick, white slurry.

Step 2 – Separation and Processing of Cassava Derivatives: Following initial processing, the starch-rich liquid phase (slurry) was separated from the insoluble fibrous material of the cassava. This was done by sieving the crushed cassava mass and pressing it through a clean microfiber cloth to extract the colloidal suspension. The collected liquid was refrigerated at 10 °C for 24 h to promote the sedimentation of starch and other solids. After the sedimentation period, the starch was fully decanted, and the supernatant, known as manipueira, was yellow. The starch was then washed multiple times with deionized water until it appeared clean and transparent (this washing water is also considered part of Manipueira). It was dried in an oven at 70 °C for 12 h, stirring every hour to ensure uniform drying. Once dried, the starch was finely ground, sieved, and stored. Similarly, the fibrous residue from the cassava root was thoroughly washed, oven-dried at 70 °C for 7 h and then ground into a fine powder before storage. The detailed steps for separating cassava derivatives are illustrated in Fig. 3.

Due to the presence of cyanogenic compounds (e.g., linamarin, lotaustralin, and hydrocyanic acid), manipueira was handled under controlled safety conditions. All procedures were conducted in a well-ventilated environment using appropriate personal protective equipment (gloves, lab coat, and safety goggles). Samples were stored at 10 °C to minimize enzymatic hydrolysis and HCN volatilization. During processing and characterization, closed or controlled systems were used whenever possible to limit exposure. Residual effluents were collected and treated in accordance with institutional safety protocols for cyanide-containing waste, thereby avoiding direct environmental discharge.

3. Characterization

The crystalline structure of the solid samples was analyzed using X-ray diffraction (XRD) with a Shimadzu XRD-6000 Powder Diffractometer (Kyoto, Japan). Measurements were performed using a Cu Kα radiation source ($\lambda = 1.5418$ Å) operating at 40 kV and 30 mA. The diffractograms were collected over a 2θ range of 3° to 80°, with a dwell time of 2 min per degree and a step size of 0.02°. The calculation of the cellulose crystallinity index (CI) was based on the Segal method (Eq. (1)), in which the maximum peak intensity $I_{(200)}$ represents the arbitrary value of the intensity peak of the crystalline parameter (200), at an angle between 22.3° and 22.7° and $I_{(am)}$ the arbitrary value of the amorphous parameter, between angles of 15°–18° (Segal et al., 1959)

$$CI\% = \frac{I_{(200)} - I_{(am)}}{I_{(200)}} \times 100\% \quad (1)$$

Fourier Transform Infrared (FTIR) spectroscopy was conducted using a Perkin-Elmer Frontier spectrometer (Boston, Massachusetts, USA) to record spectra in the range of 4000–400 cm^{-1}. Morphological and elemental analyses of the samples were performed using Scanning Electron Microscopy (SEM) on a Hitachi SU8020 microscope (Tokyo, Japan), equipped with a Thermo Scientific 4505A–6UUS-SN detector with a resolution of 134 eV.

Surface chemical composition was analyzed by X-ray photoelectron spectroscopy on a PHI Genesis instrument from Physical Electronics (Chanhassen, MN, USA), equipped with a monochromatic Al Kα X-ray source operating at 48.7 W. The pressure in the analysis chamber was 10–9 mbar, the pass energy was 27 eV, and the analysis area was 200 × 200 μm. Fitting was performed using CASAXPS (Version 2.3.26), with a Gauss-Lorentz convolution to analyze components and a Shirley background. For manipueira characterization, the sample was freeze-dried at −50 °C for 12 h using an Enterprise I freeze dryer (Terroni®, Cremona, Italy).

Thermal decomposition analysis was conducted on a METTLER TOLEDO thermogravimeter (TGA II, Greifensee, Switzerland) at a

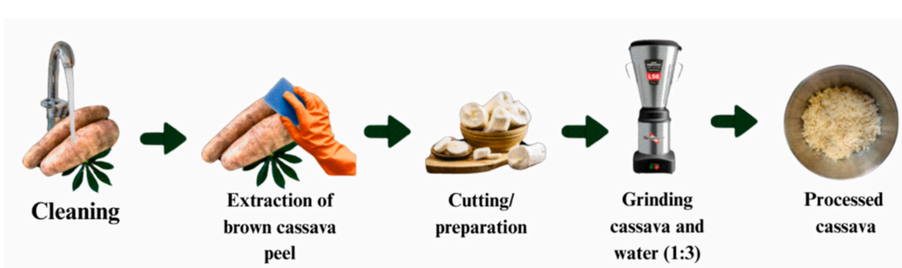

Fig. 2. Cassava cleaning and processing diagram.

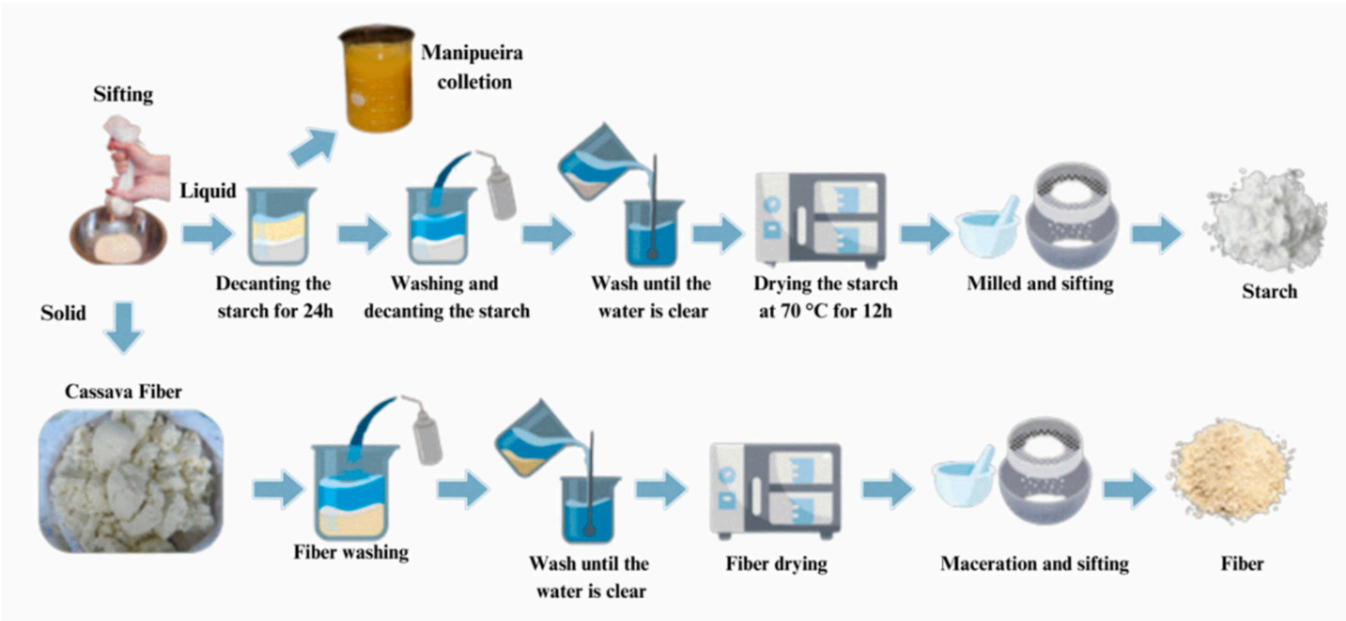

Fig. 3. Diagram showing the separation of the cassava derivatives: starch, fiber, and manipueira.

heating rate of 5 °C/min over a temperature range of 20–1000 °C. The analysis was performed under an air atmosphere at an average flow rate of 40 mL/min, using alumina supports. Moisture content was determined from the derivatives, which had been freshly collected and dried at room temperature for 24 h before analysis to avoid premature thermal alteration of the samples. It was determined in triplicate using a Shimadzu Halogen Heating Moisture Analyzer (220 V, Kyoto, Japan). Samples were heated at 107 °C for 30 min in slow mode without ramping, with an initial mass of 3 ± 0.5 g per sample. After the analysis, the samples were cooled to 30 °C, and the remaining mass was recorded for subsequent moisture calculations.

The total ash content was determined by incinerating the samples at 550–570 °C. The procedure involved carbonizing 2 g of the sample in porcelain crucibles placed on asbestos mesh and heated over a Bunsen burner flame until smoke ceased. The partially carbonized samples were then transferred to a muffle furnace and incinerated at 550 °C for approximately 6 h to ensure complete elimination of carbon. The analysis was conducted in triplicate for both cassava starch and fiber. After incineration, the crucibles containing the ash residues were cooled in a desiccator and subsequently weighed. The ash content was calculated using Eq. (2):

$$Ash\ (\%) = \left[\left(\frac{m3 - m1}{m2}\right) \times 100\right] \tag{2}$$

where m_1 is the mass of the empty crucible after drying in a muffle furnace for 30 min and cooling in a desiccator, m_2 is the initial mass of the cassava starch sample, and m_3 is the mass of the crucible containing the ash residue after incineration.

The total titratable acidity was determined by diluting 1.0 g of the sample in 50 mL of distilled water and homogenizing the mixture. From this starch or fiber solution, 10 mL was withdrawn and further diluted to 50 mL with distilled water. Two drops of phenolphthalein 1% ($C_{20}H_{14}O_4$, P.A. NEON, dissolved in ethyl alcohol 96% (Dinâmica P.A)) indicator were added, and the solution was titrated with 0.001 N sodium hydroxide (NaOH, P.A. NEON- Laderquimica) using a correction factor of 0.92 until a faint pink color was observed.

Based on the titration data, the equivalent values in grams (meq L-1) of citric acid, the main acid in cassava starch, were calculated. Additionally, the acid concentration (g L-1) and percentage (%) were determined using Eqs. (3), (4), and (5), as shown below.

$$Acidity\left(\frac{meq}{L}\right) = \frac{V.N.cf.1000}{m} \tag{3}$$

$$Acidity\ (\%) = \frac{V.N.cf.1000}{m} \times 100\% \tag{4}$$

$$Acidity\left(\frac{g}{L}\right) = \frac{V.N.cf.Eqg}{m} \tag{5}$$

where, V = volume (mL) of NaOH used in titration; N = normality of NaOH solution (0.001 N); cf = correction factor of NaOH solution; m = mass (g) or volume (mL) of sample (60 mL); Eqg = equivalent in grams of the predominant acid in the sample (Eqg = 64 (citric acid) and for manipueira Eqg = 27 (hydrocyanic acid)).

For descriptive statistical analysis, the standard deviation (Eq. (6)) was used to quantify the dispersion or variability of acidity (% and g/mL), pH, humidity, ash content, and °Brix. All parameters were analyzed in triplicate.

$$S = \sqrt{\frac{\sum (Xi - X)^2}{(n-1)}} \tag{6}$$

where X is the sample average, Xi is the individual values in the sample, and n is the count of individual values in the sample.

All analyses were carried out in triplicate, and the results were expressed as mean ± standard deviation ($n = 3$). The results were submitted to analysis of variance (ANOVA), and the average were compared via the Tukey test ($p < 0.05$).

4. Result and discussion

4.1. Evaluation of the crystalline region by XRD

The crystal structures of cassava starch, fiber, and manipueira samples were analyzed using X-ray diffraction (XRD) patterns, as shown in Fig. 4(a). The XRD pattern of cassava starch revealed a type A diffraction pattern (Aviara et al., 2016; Martens et al., 2018), which is characteristic of cereals and certain tubers. The main peaks were observed at 2θ values of 15°, 17°, and 23°, as highlighted by the arrows in the diffractogram

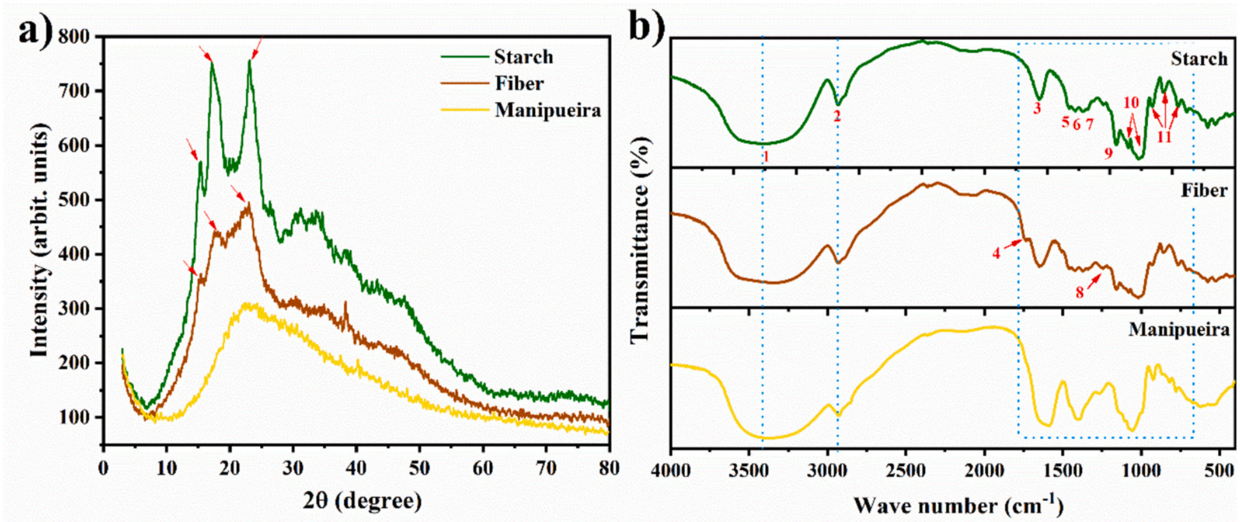

Fig. 4. X-ray Diffractograms (a) and FTIR spectra (b) of starch, fiber, and manipueira samples.

(Fig. 4a). These diffraction peaks correspond to the crystalline structure of α-amylose dihydrate. ($C_6H_{30}O_{15}.2H_2O$), as previously reported by (Weligama Thuppahige et al., 2023). For the cassava fiber sample, diffraction peaks were observed at 2θ at 16°, 17°, and 23° (Fig. 4a). Similar findings were reported in Hermiati et al. (2011) study[1], in which intense peaks at 15°, 16°, 17°, 18°, and 23° were observed in a cassava peel sample (Hermiati et al., 2011). The similarity in XRD patterns between cassava fiber and cassava starch can be attributed to the residual presence of starch in fiber after the extraction process. However, the lower intensity of the peaks corresponding to starch in the fiber sample (at 15°, 17°, and 23°) indicates a significantly reduced amount of α-amylose, likely due to the removal of starch during extraction. This observation aligns with previous findings by Hermiati et al. (2011).

In the manipueira sample, no characteristic peaks were detected, indicating the absence of starch polysaccharides and, consequently, the α-amylose polymer. This makes the sample more amorphous. This happens because amylose has a linear structure that promotes crystallization, while polymers lacking amylose or containing a high amount of highly branched polymers have less molecular organization, resulting in a more amorphous structure (Denardin and Silva, 2009).

An empirical method for determining the crystallinity of native cellulose, based on Segal's equation, was studied using X-ray diffraction (Segal et al., 1959). The crystallinity of the starch and the fiber was calculated using this method. For starch, the crystallinity index was 27.2%, and for the fiber, 26.6%.

4.2. Identification of functional groups in samples by FTIR

The FTIR spectra of the samples are shown in Fig. 4(b), and the identification and interpretation of each band are provided in Table 1. As seen in Fig. 4(b), the spectra of all samples show the absorption bands around 3300–3600, 2900–2940, 1630–1650, and 1000–1100 cm^{-1}, indicating the presence of OH, C—H, C—O—C, and C—O functional groups, respectively. Additionally, the characteristic vibration of the C—O—C ring in α 1,4 – glycosidic bonds (C—O—C) is present in the monomers of amylose and amylopectin molecules (Chen et al., 2011). The absorption band around 700–900 cm^{-1} corresponds to the vibration of the aromatic ring in C—O—C. For the cassava fiber sample (Fig. 4b), the low intensity bands at ~1730 and ~1246 cm^{-1} are associated with the carbonyl, and acetyl groups present in the hemicellulose structure (Chen et al., 2011).

Table 1
Functional groups present in starch, fiber, and manipueira samples.

No	Functional group	Wavenumber (cm^{-1})	Starch	Fiber	Manipueira
1	Stretching O—H	3600–3300	3424	3399	3368
2	Stretching C—H	2931	2932	2928	2928
3	C—O bending associated with the O—H	1637	1640	1648	1617
4	Vibration of the carbonyl group R-C=O	1739	–	1739	–
5	Symmetrical deformation CH_2	1458	1457	1469	–
6	CH_2 symmetrical scissors	1415	1418	1420	1408
7	Symmetrical C—H bending	1385–1375	1375	1378	–
8	Vibration of the acetyl group R-CH_3	1251	–	1244	1256
9	Asymmetric C—O—C stretching	1149	1160	1157	1141
10	Symmetrical C—O stretching	1200–800	1085, 1014	1078, 1014	1057
11	Ring vibration in C—O—C	920, 856, 758	927, 859, 760	931, 859, 764	922, 819, 780

4.3. Chemical characterization of the surface by XPS

The chemical composition of the samples was analyzed using X-ray photoelectron spectroscopy (XPS), with all binding energies calibrated to the carbon C 1s peak at 284.6 eV. The elements detected in the samples, along with their corresponding atomic percentages, are presented in Table 2. The results indicate that the atomic concentration of oxygen is higher in starch compared to cassava fiber. This difference can

Table 2
Atomic composition of the surface of the precursors.

Sample	Atomic concentration (%)			
	C	O	Mg	Si
Starch	59.02	40.10	0.72	0.16
Fiber	71.17	28.66	0.16	0.01
Manipueira	82.47	17.37	0.14	0.02

be attributed to the distinct molecular conformations of the two materials. Starch, primarily composed of amylose and amylopectin, exhibits more open structural configurations, exposing more oxygen atoms on its surface. Specifically, the molecular structure of amylose and amylopectin includes bonds that expose hydroxyl (-OH) groups on the glucose rings. In contrast, the cellulose-dominated structure of cassava fiber is more compact, resulting in fewer exposed oxygen atoms (Kristensen et al., 2022).

The XPS C1s spectra of the samples (Fig. 5) were deconvoluted into four components, centered at binding energies of 282.6 eV, 284.2 eV, 285.6 eV, and 287.1 eV. The component at approximately 282.6 eV corresponds to C—Si bonds, which were identified based on the presence of silicon detected in the starch sample (Szczepanik et al., 2020). The most intense component centered at 284.2 eV, is attributed to C—O—C bonds (Pandi et al., 2019). The third component, at 285.6 eV, is associated with carbon atoms in the α-position relative to a highly oxidized group (such as C═O) and with sp^2-hybridized carbons. Finally, the fourth component, centered at 287.1 eV, is related to C—O bonds and/or carbonyl groups (C═O) (Bedar et al., 2020; Carvalho et al., 2021). These spectral components confirm the presence of carboxylate groups in the cassava derivatives, as further supported by the FTIR spectra.

For the fiber, the C1s peak deconvolution revealed components

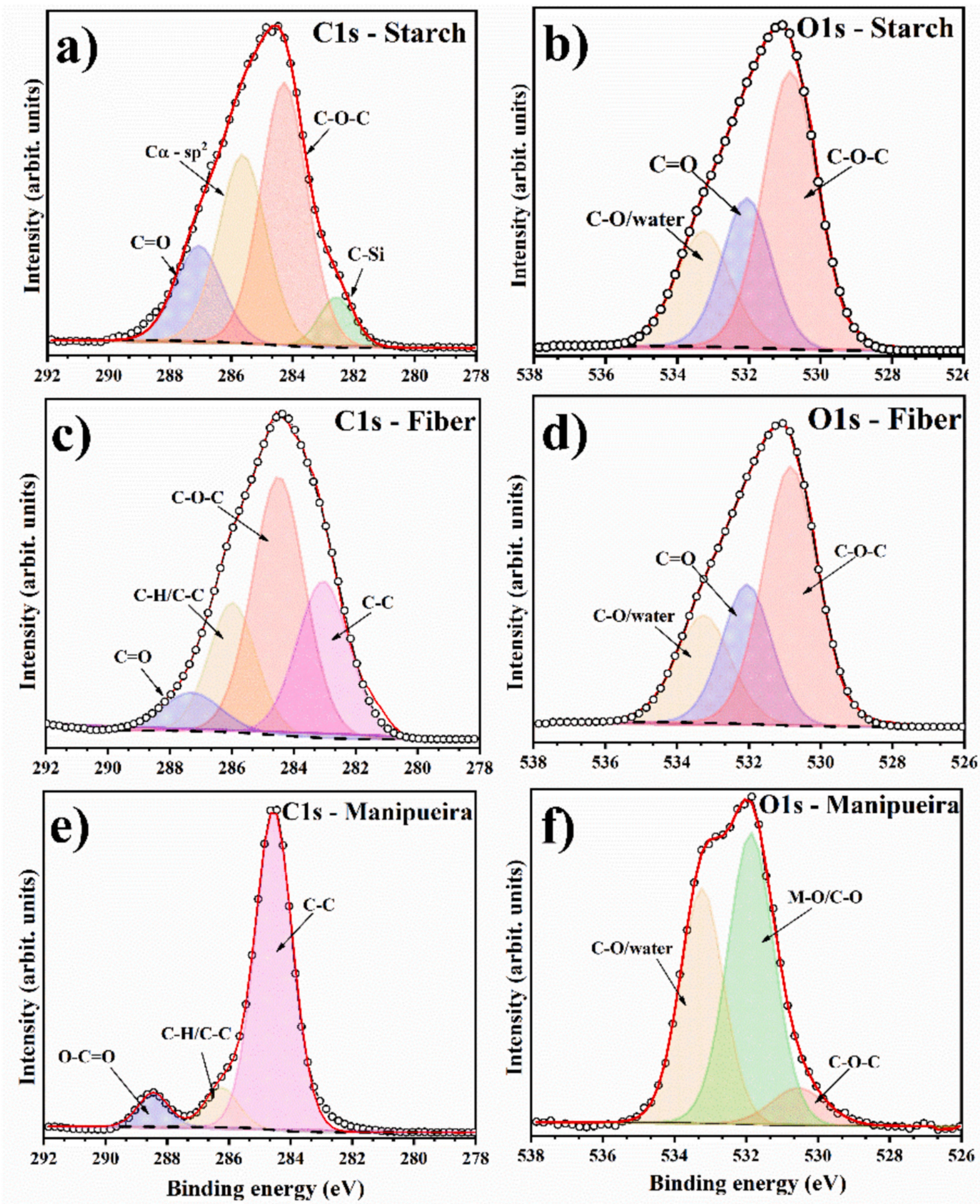

Fig. 5. XPS analysis of starch, fiber, and manipueira samples. The experimental data (open dotted) and fitted curves (solid lines) of high-resolution XPS spectra of (a) C1s (b) O1s starch; (c) C1s (d) O1s fiber; and (e) C1s (f) O1s manipueira.

related to C—C bonds at 283 eV and C—H/C—C bonds at 286.0 eV, and two more components centered at 284.6 eV (Pandi et al., 2019). The O1s spectrum of cassava starch and fiber (Fig. 5b, d) consists of three components related to the C—O bond of absorbed water at 533.0 eV, (Moreira et al., 2017), the C—O—C bonding state at 530.9 eV, (Pandi et al., 2019), and C═O species at 532.0 eV, (Guo et al., 2017). Meanwhile, for the precursor manipueira (Fig. 5f), a peak was identified at 531.8 eV, attributed to C—O bonds in metal carbonates of organic materials (Biesinger et al., 2010).

4.4. Characterization of surface morphology by SEM-EDS

Fig. 6 shows microscopy images of starch (a, b), and its corresponding histogram (Fig. 6, c) fiber (d, e, f), and manipueira (g, h, i). In the micrographs of starch (Fig. 6a and b), granules with an average size of 10.8 ± 3.5 μm (Fig. 6c) can be identified. Some of these granules are smooth and uniform with no scratches, while others have eroded surfaces with numerous cracks. According to Chen et al., 2011, the porous structure on the surface of the granules occurs due to hydrolysis or exposure to relative humidity, which creates pores and holes on the starch surface. Most cassava starch granules are truncated, which are weak points in the granule structure that increase breakability (Chen et al., 2011).

In the SEM micrographs in Fig. 6(d, e), it was observed that cassava residue fibers are mainly composed of fibrous, rough, and irregular tissue, with some holes and small granules on the fiber surfaces (Fig. 6d), which may be caused by impurities such as protein and starch granules on the fiber surface (Huang et al., 2018a). As indicated by the red arrow, the fiber pattern originating from the cellulose structure can be observed (Huang et al., 2018b). These structures had an average size of 3.7 ± 1.6 μm (Fig. 6f). The images of the manipueira sample (Fig. 6e and f) reveal an irregular surface morphology with numerous voids, large particles, and agglomerates. The manipueira sample had an average particle size of approximately 60 ± 44 μm.

4.5. Energy-dispersive spectroscopy EDS

The composition of the samples was analyzed using energy-dispersive spectroscopy (EDS), enabling semi-quantitative analysis of the chemical elements present. The results of the elemental composition are presented in Table 3. The starch sample showed only carbon and oxygen elements, while the fiber and manipueira samples included elements commonly found in cassava, especially phosphorus and

Table 3
Elemental composition (%) of starch, fiber, and manipueira detected by EDS.

Samples	Elemental composition (%)						
	C	O	Mg	P	S	Cl	K
Starch	36.0	64.0	–	–	–	–	–
Fiber	39.7	59.6	–	0.1	–	–	0.6
Manipueira	36.2	56.2	0.3	0.5	0.2	0.2	6.4

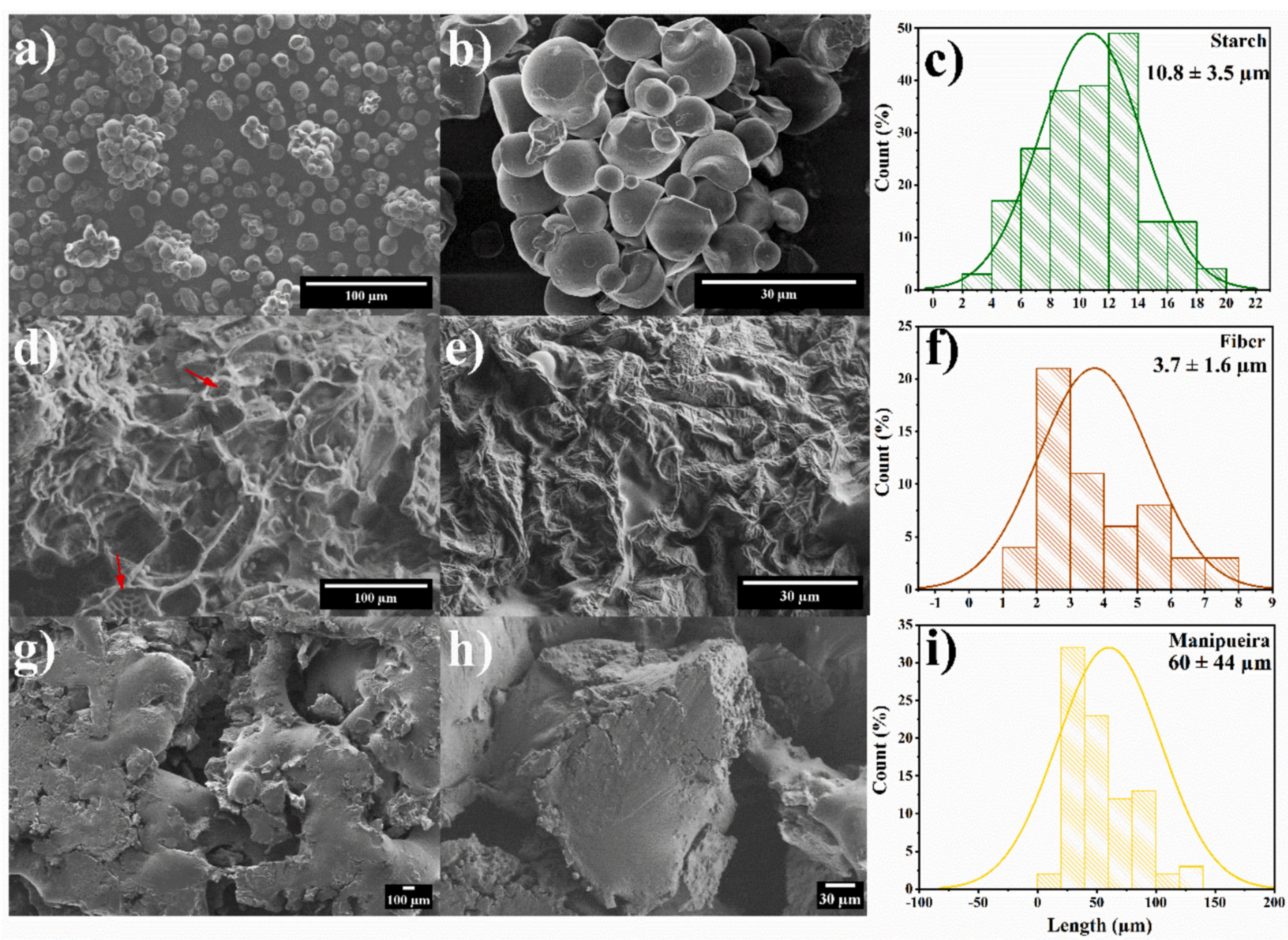

Fig. 6. SEM Micrographs of starch (a, b), fiber (d, e), and manipueira (g, h). The scale bars in the micrographs were set to 100 and 30 μm using ImageJ. The histograms show the particle size distribution for starch (c), fiber (f) and manipueira (i).

potassium. The source of these elements is mainly associated with the fertilization of the soil where the cassava was grown (Prasertsilp et al., 2023). Unlike the XPS technique, which is surface-sensitive and provides detailed information about the chemical states of elements within a few nanometers of the sample surface, EDS is a volume analysis method that offers information on the overall elemental composition of a larger sample volume. Therefore, when comparing the concentration obtained using XPS, it can be said that Mg and Si are mainly localized on the surface (Wahyuningtyas et al., 2017).

4.6. Thermogravimetric analysis of precursors (TG/DTA)

Thermogravimetric analysis was performed to evaluate the thermal stability of the samples over the temperature range 25–1000 °C. Fig. 7 shows the thermogravimetric (TG) and derivative thermogravimetric (DTG) curves for starch, fiber, and manipueira. Stage 1 involves mass loss corresponding to humidity release, occurring at temperatures between 30° and 130 °C. During this stage, there is also a loss of very light volatile compounds, and the process of thermal decomposition begins as water evaporates (Shanks and Kong, 2012). Stage 2 refers to the process of volatile matter release that occurs between 130 °C and 380 °C. This is the main stage of thermal decomposition, characterized by a significant loss of material, especially amylose, which can be transformed into carbohydrate lipids, composed of carbon, hydrogen, and oxygen (Shanks and Kong, 2012). Cassava starch (Fig. 7a) begins to decompose thermally at 300 °C. This stage causes rapid thermal decomposition, resulting in significant mass loss, which is accelerated by the considerable oxygen content in the starch and fiber samples, as evidenced by XPS data.

Stage 3 occurs after the release of volatile matter in the samples at temperatures between 380 and 530 °C. At this stage, coal is flammable because it is surrounded by volatile matter, and oxygen diffuses on the surface of the carbon, burning it simultaneously with the volatile matter. This stage is when residual coal from the fiber is formed (Melo et al., 2023). After 400 °C, both for starch and fiber (Fig. 7b), the rate of mass loss stabilizes, and from this point onwards, the fixed carbon combusts (Da Cruz et al., 2021; Melo et al., 2023). In the case of manipueira (Fig. 7c), the final stage of thermal decomposition occurred between 530 °C and 800 °C. The thermal event observed between 530 and 800 °C is attributed to a combination of processes involving the decomposition and transformation of inorganic species present in the sample. This stage may include the decomposition of intermediate carbonate species and the breakdown of residual inorganic salts (Baudin et al., 2023). This interpretation is supported by EDS results, which revealed the presence of elements such as K, Mg, P, S, and Cl, suggesting the occurrence of compounds including carbonates, phosphates, sulfates, and chlorides, all of which may undergo thermal transformations within this temperature range.

Table 4 shows the events for each sample, along with the exact temperature calculated from the derivative. Based on the mass used for analysis, the total percentage of sample combustion was determined, revealing that starch undergoes almost 100% combustion in only two thermogravimetric events. This characteristic is advantageous in syntheses because it indicates that nearly all starch will be consumed and converted into fuel for the reaction.

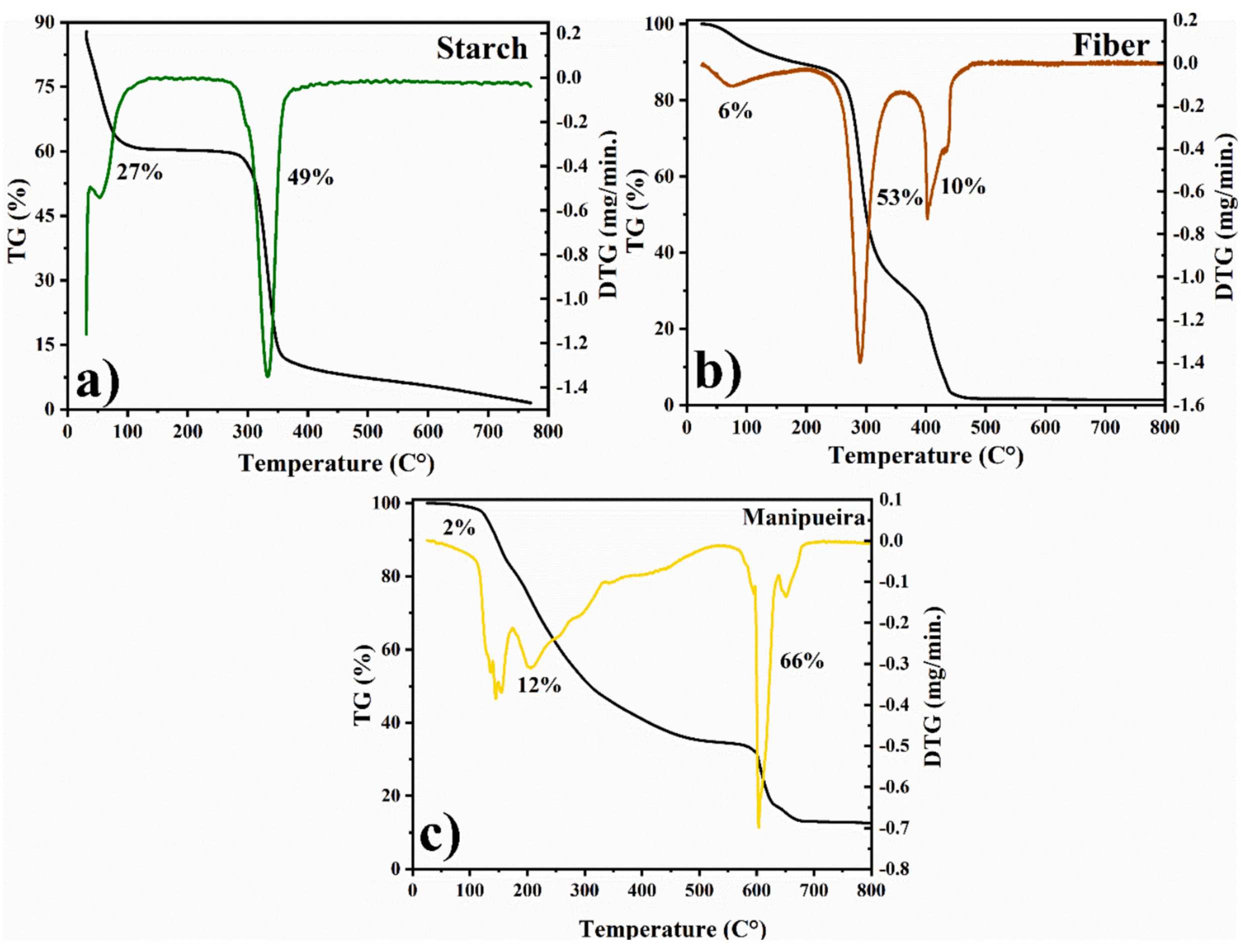

Fig. 7. TG/DTG thermal decomposition of samples (a) starch, (b) fiber, and (c) manipueira. The curves of samples were obtained by scanning from 20° to 1000 °C in an air atmosphere with a flow rate of 40 mL·min^{-1} and a heating rate of 5 °C/min.

Table 4
Respective masses used for analysis, mass loss event, temperature, and percentage of mass loss.

Samples	Mass for analysis (mg)	Loss of mass events (C°)	Temperature DTG	Mass loss (%)	Total sample burning (%)
Starch	14.3167	30–130	54	27	99.9
		130–380	330	49	
Fiber	17.6015	30–130	72.4	6	93.5
		130–380	289	53	
		380–530	412	8	
Manipueira	16.9920	30–130	126	2	93.2
		130–380	207	12	
		530–800	605	66	

4.7. Determination of total titratable acidity (g L^{-1} and %)

The data obtained for acidity percentage, pH, and humidity were analyzed for all samples. Ash analyses were performed only on the starch and fiber samples because of the high moisture content of the manipueira sample (Table 5). The analysis was compared with Brazilian legislation from the Ministry of Agriculture, Livestock and Supply, NORMATIVE INSTRUCTION No. 52, OF 7 NOVEMBER 2011, which was compared with standard CXS 176-1989, Standard for Edible Cassava Flour.

According to standard 52/2011, the acidity index classifies starch as sweet for acidity values between 1.0 and 3.0%, and as sour for values between 3.1 and 5.0%. Therefore, based on these standards, the analyzed starch sample is classified as a sweet starch, since the average acidity of the three samples is 1.58%. The average pH was 5.77, with the minimum and maximum limits set at 3.0 and 7.0, both of which were met. Ash is the fixed mineral residue resulting from incinerating the product sample, and values exceeding the maximum tolerance allowed by Normative Instruction 52/2011—less than or equal to 1.4%—are associated with significant levels of Ca, P, Fe, and Mg, as well as indicating contamination by foreign material in the product caused by failures during some stages of processing.

The average mineral residue (ash) content for starch was 0.13%, in accordance with Normative Instruction 52/2011 (≤1.4%) and CXS 176-1989 Standard by Codex Alimentarius (max. 3.0%).

According to the same standard 52/2011, based on the acidity levels in the cassava flour sample, acidity up to 3.0% is considered low, while above 3.0% is considered high, falling into the dry and bijusada groups. The average acidity of the triplicate fiber samples was 2.30%, classified as low titratable acidity. pH is a key factor in limiting microbial growth in food. Based on this parameter, samples can be classified as slightly acidic (pH > 4.5), acidic (pH 4.5 to 4.0), and very acidic (pH < 4.0) (Chisté and Cohen, 2011). Based on this classification, the analyzed cassava fiber was considered slightly acidic, with an average pH above 4.5. The average ash content of the fiber was 0.53%. Both samples exhibited low ash levels, indicating a low mineral content in the starch and fiber studied.

The values for total titratable acidity were lower than those reported by (Chisté and Cohen, 2011) who studied the fermentation of manipueira in the preparation of tucupi, a yellow, acidic, and aromatic slurry extracted from bitter cassava that is essential in Amazonian cuisine. It forms the base for iconic dishes such as Tacacá and Pato no Tucupi. The study reports that the increase in total acidity is associated with a decrease in pH during tucupi processing, due to acid release during fermentation. In simple terms, the fermentation of the starch present seems to be responsible for the increase in acidity; the higher the acidity, the more intense the fermentation or the longer the maceration process.

The pH of manipueira plays an important role in determining its chemical stability and reactivity as a precursor medium. Under slightly acidic to near-neutral conditions (pH 3.5–6.5), cyanogenic compounds such as linamarin may undergo partial hydrolysis, generating reactive species, including hydrocyanic acid and carbonyl compounds (Brito et al., 2023). These transformations can modify the chemical environment by introducing additional functional groups and influencing redox behavior (Brito et al., 2023; Padayatchee et al., 2025). From a materials synthesis perspective, such pH-dependent changes are relevant, as they affect interactions with metal ions, precursor stability, and decomposition pathways during thermal or combustion-assisted processes, which are key factors controlling the physicochemical properties of the resulting materials (Padayatchee et al., 2025). Therefore, the measured pH (6.54) indicates a condition close to the upper stability limit of these transformations, supporting the use of manipueira as a moderately reactive liquid precursor. This interpretation is consistent with the FTIR and TGA results, which indicate the presence of reactive functional groups and thermally active components in manipueira.

Regarding soluble solids content (°Brix), the value for manipueira was 1.3, which is relatively low. The soluble solids content indicates, among other constituents, the sugars dissolved in the medium, which are also available for fermentation; this may explain the decrease in content during the fermentation of manipueira. The content of fermented tucupi after the cooking process can reach up to 8.1°Brix (Marney, 2001).

In terms of moisture content, this study examined the relative moisture content of cassava derivatives. The fiber content was similar to that reported in the literature for samples dried at room temperature and post-processing (Chen et al., 2024), at approximately 55.3%. As for starch, values reported in the literature ranged from 10 to 14% (Basha et al., 2021) which is consistent with the value found in this study. The moisture content of cassava directly influences the efficiency of starch extraction; a higher moisture content improves the solubilization and separation of starch during extraction, thereby increasing overall efficiency (Chen et al., 2024). Since the manipueira is a liquid, its humidity was high (99.7%), resulting in a low percentage of total solids for these values (Primo et al., 2019). The relative moisture content of the samples can also be determined using FTIR techniques in the 3600–3300 cm^{-1} band and by the first-stage mass loss at 30–130 °C via thermogravimetric analysis.

Statistical differences among the samples were evaluated using ANOVA followed by Tukey's test. For acidity %, fiber differed significantly from starch and manipueira, while the latter two showed no significant difference. In contrast, pH and moisture values differed significantly across all samples, indicating distinct physicochemical environments and compositions.

The characterization of the three derivatives of cassava: starch, fiber, and manipueira reveals structural, thermal, chemical, and morphological differences that influence their potential uses as organic precursors in material synthesis, especially for metal oxides, films, carbons, and hybrid composites (Balaba et al., 2023; Edhirej et al., 2017; Pari et al., 2014; Primo et al., 2020). The starch exhibited a type A crystalline pattern, typical of semi-crystalline materials with a certain level of

Table 5
Determination of acidity, ash content, pH, moisture content, and °Brix for the starch, fiber, and manipueira samples. Different letters in the same column indicate statistically significant differences according to Tukey's test ($p < 0.05$).

Samples	Acidity (%)	Acidity (g/mL)	pH	Moisture content (%)	Ashes (%)	Soluble solids (°Brix)
Starch	1.58 ± 0.09^{a}	0.00101 ± 0.00005^{a}	5.77 ± 0.11^{a}	13.3 ± 0.25^{a}	0.134 ± 0.07^{a}	–
Fiber	2.30 ± 0.15^{b}	0.00147 ± 0.0001^{a}	4.68 ± 0.07^{b}	55.3 ± 5.24^{b}	0.530 ± 0.03^{b}	–
Manipueira	1.64 ± 0.35^{a}	0.04416 ± 0.0096^{b}	6.54 ± 0.04^{c}	99.7 ± 0.07^{c}	–	1.334 ± 0.00

amylopectin, as evidenced by well-defined peaks in the X-ray diffractogram and numerous hydroxyl groups seen in the FTIR. This organized structure promotes gelation, metal ion complexation, and the formation of ordered matrices (Ferreira et al., 2022; Varma et al., 2016), which makes starch an excellent molding agent and fuel in synthesis methods such as self-combustion, biopolymer sol–gel, and edible films, offering advantages for food packaging and nanometric oxide formation (Mastalska-Popławska et al., 2020; Mastuli et al., 2014; Pei et al., 2024). EDX analysis showed that the starch in the three samples contained only C and O, or very low concentrations of other elements, making it ideal for synthesis. The TGA results indicated that starch nearly decomposes completely up to 380 °C, producing minimal ash and releasing a large volume of volatiles, which is essential for obtaining high-purity oxides and porous morphology after calcination (Alyson et al., 2018; Ananda et al., 2021; Mastalska-Popławska et al., 2020). SEM images highlight their potential, as eroded and microcracked granules provide a larger active surface area and enhance the diffusion of metallic precursors within the organic matter matrix (Mastalska-Popławska et al., 2020).

Cassava fiber, in contrast, displayed characteristics of cellulose, hemicellulose, and lignin, as observed by FTIR and XPS. These macromolecules give the fiber a more rigid, aromatic structure, leading to increased thermal stability and three distinct stages of thermal decomposition. The presence of inorganic residues such as K, Mg, and P, identified by EDX, indicates that these derivatives retain soil minerals, which can act as activators during carbonization (Hamissou et al., 2023; Huang et al., 2018b). Morphologically, the fiber has a rough, irregular surface with well-defined channels and fibrillar structures visible under SEM. This surface topography promotes the anchoring of metallic nanoparticles and supports the formation of fiber–oxide composites and high-surface-area activated carbon materials (Bolaños et al., 2025; Da Cruz et al., 2021; Guan et al., 2025; Kayiwa et al., 2021). Thus, the fiber stands out as a precursor for producing structural carbons, adsorbents, doped materials, and catalytic supports containing dispersed ceramic phases.

Manipueira, on the other hand, is characterized by its completely amorphous nature, as confirmed by X-ray compared to other cassava derivatives, and by its complex composition, which includes soluble carbohydrates, proteins, glycosides, mineral salts, and cyanogenic compounds (de Queiroz et al., 2020; Maciel et al., 2023). FTIR spectra indicated the presence of OH, C—O, carbonyl, and C—O—C groups, which enhance interactions with metal cations and support organic-inorganic synthesis methods. The TGA results showed a final decomposition phase between 530 and 800 °C, attributed to the breakdown of non-volatile oxides and the formation of more stable inorganic residues, confirming its potential as a substrate in various processes and mixed-phase synthesis (Maia et al., 2023; Matsui et al., 2004; Melo et al., 2023). Because of its liquid nature, manipueira can also serve as a dispersing medium, organic binder, and reducing agent in sol-gel synthesis and assisted combustion (Dugganaboyana et al., 2025; Prabhakaran et al., 2025). When integrated, these results demonstrate that the three cassava derivatives are functionally complementary for materials production. Starch is a highly pure and efficient precursor for forming metal oxide nanoparticles due to its semi-crystalline structure, high thermal reactivity, and low waste generation.

The fiber, rich in lignocellulosic structures and mineral elements, has greater thermal stability and is ideal for producing structural carbons, catalytic supports, and hybrid composites. Manipueira, in turn, acts as an amorphous, multifunctional liquid precursor, capable of facilitating combustion synthesis routes or being used as a fertilizer. This diversity in thermal, chemical, and structural behaviors enables the development of versatile and sustainable routes for advanced materials, significantly expanding the use of cassava as high-value biomass in materials engineering. The data in Table 6 demonstrate that each cassava derivative plays a distinct functional role, reinforcing their complementary potential in integrated and sustainable material synthesis strategies.

Table 6
Summary of reported applications of cassava derivatives highlighting their functional roles in material synthesis, biotechnology, and agriculture.

Cassava derivative	Application type	Role in process	Key outcome	Reference
Starch	Oxide synthesis	Fuel and gelling agent	Synthesis of ZnO (pigments)	(Primo et al., 2019)
			Synthesis of MgO (ions adsorption)	(Balaba et al., 2024)
			Synthesis of CuO NPs (Biomedical applications)	(Pei et al., 2026; Sugumar et al., 2025)
Starch	Polymer films	Matrix former	Transparent, flexible biodegradable films	(Parra et al., 2004)
Fiber	Carbon materials	Structural precursor	Activated carbon with a high surface area	(Pari et al., 2014)
Fiber	Nanomaterials	Cellulose source	Cellulose whiskers for nanocomposites	(Edhirej et al., 2017)
Fiber	Composites	Reinforcement phase	Improved mechanical properties (cardboard-like material)	(Matsui et al., 2004)
Manipueira	Agriculture	Organic fertilizer	Nutrient supply for sunflower growth	(Dantas et al., 2017)
Manipueira	Biotechnology	Fermentation substrate	Production of carotenoids via yeast	(Maia et al., 2023)

5. Conclusion

The results demonstrate that the derivatives obtained from cassava wet processing exhibit distinct physicochemical and structural features that directly influence their behavior as precursors for materials synthesis. Starch presented a semi-crystalline structure with defined granule morphology and low ash content, indicating high purity and suitability for controlled thermal conversion and templating applications. Fiber exhibited a typical lignocellulosic composition, as confirmed by FTIR and thermal analyses, which contributed to enhanced thermal stability and the potential for carbon-rich material formation. Manipueira showed a complex chemical composition, including dissolved organic matter and reactive species, as evidenced by its physicochemical parameters and spectroscopic signatures. Its pH and compositional profile suggest a chemically active medium that can interact with metal ions and influence precursor stability and decomposition pathways during thermal and combustion-assisted synthesis. Thermogravimetric analysis revealed distinct decomposition stages for each derivative, reflecting their different organic compositions and confirming their potential for thermal processing. Surface and structural analyses further support the presence of functional groups capable of participating in coordination, redox reactions, and carbonization processes. Unlike conventional approaches that focus on a single residue, this study adopts an integrated strategy in which all derivatives obtained from the same processing route are simultaneously recovered, characterized, and evaluated as functional precursors. This approach enables a more comprehensive and consistent valorization of cassava biomass, supporting circular and low-impact material development.

CRediT authorship contribution statement

Nayara Balaba: Writing – review & editing, Writing – original draft, Methodology, Investigation, Formal analysis, Conceptualization. **Julia de Oliveira Primo:** Writing – original draft, Validation, Methodology, Conceptualization. **Xavier Noirfalise:** Validation. **Luiz Felipe Bodnar:** Validation, Methodology, Investigation. **Rafael Emil Klumpp:** Writing – review & editing. **Carla Bittencourt:** Writing – review & editing, Supervision. **Fauze Jaco Anaissi:** Writing – review & editing, Supervision, Project administration.

Declaration of competing interest

The authors declare the following financial interests/personal relationships which may be considered as potential competing interests: Nayara Balaba reports financial support was provided by Coordination for the improvement of Higher Education Personnel. Fauze Jaco Anaissi reports financial support was provided by Coordination for the improvement of Higher Education Personnel. Fauze Jaco Anaissi reports financial support was provided by National Council for Scientific and Technological Development. Nayara Balaba reports financial support was provided by Wallonie-Bruxelles International. Nayara Balaba reports financial support was provided by Araucaria Foundation. Nayara Balaba reports a relationship with Coordination for the improvement of Higher Education Personnel that includes: funding grants. Fauze Jaco Anaissi reports a relationship with Coordination for the improvement of Higher Education Personnel that includes: funding grants. Fauze Jaco Anaissi reports a relationship with National Council for Scientific and Technological Development that includes: funding grants. Nayara Balaba reports a relationship with Araucaria Foundation that includes: funding grants. Nayara Balaba reports a relationship with Wallonie-Bruxelles International that includes: funding grants. If there are other authors, they declare that they have no known competing financial interests or personal relationships that could have appeared to influence the work reported in this paper.

Acknowledgments

Balaba appreciates Capes for a graduate scholarship. Anaissi is thankful for a CNPq Productivity grant (310815/2022-3) and the CNPq grant (427127/2018-1). Anaissi and Bittencourt are grateful for a WBI/Confap-Fundação Araucária (BEL2023081000001).

Data availability

Data will be made available on request.

References

Alyson, L.P.R., Glauber, C., Maria, E.P.S., Wolia, C.G., 2018. Application of cassava harvest residues (Manihot esculenta Crantz) in biochemical and thermochemical conversion process for bioenergy purposes: a literature review. Afr. J. Biotechnol. 17, 37–50. https://doi.org/10.5897/AJB2017.16322.

Ananda, A., Ramakrishnappa, T., Archana, S., Yadav, L.S.R., Shilpa, B.M., Nagaraju, G., Jayanna, B.K., 2021. Green synthesis of MgO nanoparticles using *Phyllanthus emblica* for Evans Blue degradation and antibacterial activity. Mater. Today Proc. https://doi.org/10.1016/j.matpr.2021.05.340.

Aviara, N.A., Chukwugoziem Igbeka, J., Nwokocha, L., 2016. Effect of Drying Temperature on Physicochemical Properties of Cassava Starch.

Balaba, N., Horsth, D.F.L., Correa, J. de S., Primo, J. de O., Jaerger, S., Alves, H.J., Bittencourt, C., Anaissi, F.J., 2023. Eco-friendly polysaccharide-based synthesis of nanostructured MgO: application in the removal of Cu2+ in wastewater. Materials 16, 1–15. https://doi.org/10.3390/ma16020693.

Balaba, N., Primo, J. de O., Sotiles, A.R., Jaerger, S., Horsth, D.F.L., Bittencourt, C., Anaissi, F.J., 2024. Synthesis of Periclase phase (MgO) from colloidal Cassava starch suspension, dual application: Cr(III) removal and pigment reuse. PhysChem 4, 61–77. https://doi.org/10.3390/physchem4010005.

Basha, R.K., Leong, K.Y., Othman, S.H., Talib, R.A., Naim, M.N., Hasnan, N.Z.N., Azmi, N.S., 2021. Sorption characteristic of starch-based film. Food Res. 5 (S1), 193–200. https://doi.org/10.26656/fr.2017.5(S1).056.

Baudin, F., Bouton, N., Wattripont, A., Carrier, X., 2023. Carbonates thermal decomposition kinetics and their implications in using Rock-Eval® analysis for carbonates identification and quantification. Sci. Technol. Energy Transit. 78, 38. https://doi.org/10.2516/stet/2023038.

Bedar, A., Goswami, N., Singha, A.K., Kumar, V., Debnath, A.K., Sen, D., Aswal, V.K., Kumar, S., Dutta, D., Keshavkumar, B., Ghodke, S., Jain, R., Singh, B.G., Tewari, P. K., Bindal, R.C., Kar, S., 2020. Nanodiamonds as a state-of-the-art material for enhancing the gamma radiation resistance properties of polymeric membranes. Nanoscale Adv. 2, 1214–1227. https://doi.org/10.1039/C9NA00372J.

Biesinger, M.C., Lau, L.W.M., Gerson, A.R., Smart, R.St.C, 2010. Resolving surface chemical states in XPS analysis of first row transition metals, oxides and hydroxides: Sc, Ti, V, Cu and Zn. Appl. Surf. Sci. 257, 887–898. https://doi.org/10.1016/j.apsusc.2010.07.086.

Bolaños, P.A., Buitron, E.S.C., Carlosama, D.E., Muñoz, R.C., Castillo, H.S.V., Rodriguez, G.A.T., 2025. Development of a biocomposite based on cassava bagasse and fique fiber with potential use in the manufacture of pots: physical–mechanical characterization and biodegradability. Cellulose 32, 4249–4270. https://doi.org/10.1007/s10570-025-06484-0.

Brito, G.F., Agrawal, P., Araujo, E.M., Melo, J.J.A., 2011. Biopolímeros, polímeros biodegradáveis e polímeros verdes. Rev. Eletron. Mater. Processos 6, 127–139 doi:1809-8797.

Brito, B.d.N.d.C., Martins, M.G., Chisté, R.C., Lopes, A.S., Gloria, M.B.A., Pena, R.d.S., 2023. Total and free hydrogen cyanide content and profile of bioactive amines in commercial Tucupi, a traditionally derived cassava product widely consumed in Northern Brazil. Foods 12 (23), 4333. https://doi.org/10.3390/foods12234333.

Carvalho, A., Costa, M.C.F., Marangoni, V.S., Ng, P.R., Nguyen, T.L.H., Castro Neto, A.H., 2021. The degree of oxidation of graphene oxide. Nanomaterials 11, 560. https://doi.org/10.3390/nano11030560.

Chen, Y., Huang, S., Tang, Z., Chen, X., Zhang, Z., 2011. Structural changes of cassava starch granules hydrolyzed by a mixture of α-amylase and glucoamylase. Carbohydr. Polym. 85, 272–275. https://doi.org/10.1016/j.carbpol.2011.01.047.

Chen, L., Li, K., Mou, X., Liu, Z., Jiang, H., Mabrouk, M., Pan, J., Atwa, E.M., 2024. Evaluating the impact of moisture content and loading orientation on the geometrical characteristics and mechanical behavior of cassava tubers. Agronomy 14 (10), 2254. https://doi.org/10.3390/agronomy14102254.

Chisté, R.C., Cohen, K. de O., 2011. Total and free cyanide content in the processing steps of tucupi. Rev. Inst. Adolfo Lutz 70, 41–46. https://doi.org/10.53393/rial.2011.v70.32589.

Da Cruz, M.A., Casanova, R.F., Boscardin, D., Zanchet, A., 2021. Analysis of the influence of calcination temperature of sugarcane residues for the production of binders. Rev. Mater. 26. https://doi.org/10.1590/S1517-707620210004.1313.

Dantas, M.S.M., Rolim, M.M., Bonfim-Silva, E.M., Pedrosa, E.M.R., Silva, Ê.F.F. e, da Silva, G.F., 2017. The use of "manipueira" wastewater derived from cassava processing as organic fertilizer in sunflower cultivation. Aust. J. Crop Sci. 861–867. https://doi.org/10.21475/ajcs.17.11.07.pne508.

Denardin, C.C., Silva, L.P. da, 2009. Structure of starch granules and their relationship with physicochemical properties. Ciência Rural 39, 945–954. https://doi.org/10.1590/S0103-84782009005000003.

Dugganaboyana, G.K., Gunjevu Kannankumar, M.K., Shivaramakrishna, S., Vani Raju, M., Kaniyur Chandrasekaran, M., Muthaiyan Ahalliya, R., Panneerselvam, N., Palanisamy, C.P., Velliyur Kanniappan, G., 2025. Phytochemical insights, antioxidant activity and therapeutic potential of Cassia senna against prostate cancer in Wistar albino rats. Discov. Appl. Sci. 7 (10), 1206. https://doi.org/10.1007/s42452-025-07392-5.

Edhirej, A., Sapuan, S.M., Jawaid, M., Zahari, N.I., 2017. Cassava: its polymer, fiber, composite, and application. Polym. Compos. 38, 555–570. https://doi.org/10.1002/pc.23614.

Ferreira Filho, J.R., Silveira, H.F., Macedo, J.J.G., Lima, M.B., Cardoso, C.E., 2013. Cultivo, processamento e uso da mandioca: Instruções práticas. Brasilia, DF.

Ferreira, P.P.L., Melo, D.M. de A., Medeiros, R.L.B. de A., de Araújo, T.R., Maziviero, F. V., de Oliveira, Â.A.S., 2022. Green synthesis with Aloe Vera of MgAl2O4 substituted by Mn and without calcination treatment. Res. Soc. Dev. 11, e14411628873. https://doi.org/10.33448/rsd-v11i6.28873.

Guan, T., Gong, J., Lin, J., Palanisamy, C.P., Pei, J., Abd El-Aty, A.M., 2025. Machine learning-driven multimodal optimization of selenium biotransformation and flavor profiling in fermented apple–Yacon functional beverages. Innovative Food Sci. Emerg. Technol. 105, 104198. https://doi.org/10.1016/j.ifset.2025.104198.

Guo, L.Q., Qin, S.X., Yang, B.J., Liang, D., Qiao, L.J., 2017. Effect of hydrogen on semiconductive properties of passive film on ferrite and austenite phases in a duplex stainless steel. Sci. Rep. 7. https://doi.org/10.1038/s41598-017-03480-8.

Guo, H., Liu, Y., Wan, T., Song, D., Palanisamy, C.P., Geng, J., Pei, J., Özmen, S., Abd El-Aty, A.M., 2024. Toward personalized cancer management: role of precision nutrition–diet interventions. J. Funct. Foods 123, 106584. https://doi.org/10.1016/j.jff.2024.106584.

Hamissou, I.G.M., Appiah, K.E.K., Sylvie, K.A.T., Ousmaila, S.M., Casimir, B.Y., Benjamin, Y. kouassi, 2023. Valorization of cassava peelings into biochar: physical and chemical characterizations of biochar prepared for agricultural purposes. Sci. Afr. 20, e01737. https://doi.org/10.1016/j.sciaf.2023.e01737.

Hermiati, E., Azuma, J., Mangunwidjaja, D., Sunarti, T.C., Suparno, O., Prasetya, B., 2011. Hydrolysis of carbohydrates in cassava pulp and tapioca flour under microwave irradiation. Indian J. Chem. 11, 238. https://doi.org/10.22146/ijc.21387.

Huang, L., Zhang, X., Xu, M., An, S., Li, C., Huang, C., Chai, K., Wang, S., Liu, Y., 2018a. Dietary fibres from cassava residue: physicochemical and enzymatic improvement, structure and physical properties. AIP Adv. 8. https://doi.org/10.1063/1.5054639.

Huang, L., Zhang, X., Xu, M., Chen, J., Shi, Y., Huang, C., Wang, S., An, S., Li, C., 2018b. Preparation and mechanical properties of modified nanocellulose/PLA composites from cassava residue. AIP Adv. 8. https://doi.org/10.1063/1.5023278.

Jayaraman, S., Eswaran, A., Rajagopal, P., Palanisamy, C.P., Veerakumar, P., Veeraraghavan, V.P., Sirasanagandla, S.R., 2026. Neuroendocrine-associated epigenetic factors in cellular senescence: mechanisms and therapeutic implications. Biogerontology 27 (2), 64. https://doi.org/10.1007/s10522-026-10402-7.

Jiang, H., Kumarasamy, R.V., Pei, J., Raju, K., Kanniappan, G.V., Palanisamy, C.P., Mironescu, I.D., 2025. Integrating engineered nanomaterials with extracellular vesicles: advancing targeted drug delivery and biomedical applications. Front. Nanotechnol. 6. https://doi.org/10.3389/fnano.2024.1513683.

Jorge, F.-F., Edith, C.-C., Eduardo, R.-S., Jairo, S.-M., Héctor, C.-V., 2023. Hydrothermal processes and simultaneous enzymatic hydrolysis in the production of modified cassava starches with porous-surfaces. Heliyon 9, e17742. https://doi.org/10.1016/j.heliyon.2023.e17742.

Kannappan, P., Kaniyur Chandrasekaran, M., Vani Raju, M., Gopalakrishnan, S., Dhamodharan, P., Muthaiyan Ahalliya, R., Palanisamy, C.P., Raju, B., Velliyur Kanniappan, G., 2025. Exploring the anticancer potential of Jerantinine A from *Tabernaemontana coronaria* against prostate, breast, and ovarian cancers: a computational approach. J. Complement. Integr. Med. 22 (2), 363–372. https://doi.org/10.1515/jcim-2024-0443.

Kayiwa, R., Kasedde, H., Lubwama, M., Kirabira, J.B., 2021. Mesoporous activated carbon yielded from pre-leached cassava peels. Bioresour. Bioprocess. 8, 53. https://doi.org/10.1186/s40643-021-00407-0.

Khejornsart, P., Meenongyai, W., Juntanam, T., 2022. Cassava pulp added to fermented total mixed rations increased tropical sheep's nutrient utilization, rumen ecology, and microbial protein synthesis. J. Adv. Vet. Anim. Res. 9, 754–760. https://doi.org/10.5455/JAVAR.2022.I645.

Kristensen, K., Warne, G., Agarwal, D., Foster, T.J., 2022. Effects of different moisture contents on the structural and functional properties of cellulose with cell wall components in different citrus fibres. Food Funct. 13, 2756–2767. https://doi.org/10.1039/D1FO02808A.

Kumarasamy, R.V., Natarajan, P.M., Umapathy, V.R., Roy, J.R., Mironescu, M., Palanisamy, C.P., 2024. Clinical applications and therapeutic potentials of advanced nanoparticles: a comprehensive review on completed human clinical trials. Front. Nanotechnol. 6. https://doi.org/10.3389/fnano.2024.1479993.

Li, M., Xu, J., Cai, Z., Zhu, P., Liu, K., Deng, S., Li, Y., Fan, X., 2026. Variations in carbon flux allocation among cassava (*Manihot esculenta*) cultivars arise from balanced competition between starch accumulation and structural component development. Commun. Biol. 9 (1), 277. https://doi.org/10.1038/s42003-026-09556-4.

Maciel, A.C., da Silva Pena, R., do Nascimento, L.D., de Oliveira, T.A., Chagas-Junior, G.C.A., Lopes, A.S., 2023. Health exposure risks and bioremediation of cyanide in cassava processing effluents: an overview. J. Water Process Eng. 55, 104079. https://doi.org/10.1016/j.jwpe.2023.104079.

Maia, F. de A., Igreja, W.S., Xavier, A.A.O., Mercadante, A.Z., Lopes, A.S., Chisté, R.C., 2023. Concentrated Manipueira as an alternative low-cost substrate to *Rhodotorula glutinis* for biotechnological production of high contents of carotenoids. Fermentation 9, 617. https://doi.org/10.3390/fermentation9070617.

Marney, C.P., 2001. Management use and treatment of by-products from the industrialization of cassava -vol-4, 4. Fundação Cargill, pp. 1–320.

Martens, B.M.J., Gerrits, W.J.J., Bruininx, E.M.A.M., Schols, H.A., 2018. Amylopectin structure and crystallinity explains variation in digestion kinetics of starches across botanic sources in an in vitro pig model. J. Anim. Sci. Biotechnol. 9. https://doi.org/10.1186/s40104-018-0303-8.

Mastalska-Popławska, J., Sikora, M., Izak, P., Góral, Z., 2020. Role of starch in the ceramic powder synthesis: a review. J. Solgel Sci. Technol. 96, 511–520. https://doi.org/10.1007/s10971-020-05404-x.

Mastuli, M.S., Kamarulzaman, N., Nawawi, M.A., Mahat, A.M., Rusdi, R., Kamarudin, N., 2014. Growth mechanisms of MgO nanocrystals via a sol-gel synthesis using different complexing agents. Nanoscale Res. Lett. 9, 1–9. https://doi.org/10.1186/1556-276X-9-134.

Matsui, K.N., Larotonda, F.D.S., Paes, S.S., Luiz, D.B., Pires, A.T.N., Laurindo, J.B., 2004. Cassava bagasse-Kraft paper composites: analysis of influence of impregnation with starch acetate on tensile strength and water absorption properties. Carbohydr. Polym. 55, 237–243. https://doi.org/10.1016/j.carbpol.2003.07.007.

Melo, I.K.L., Tavares, M.C., da Silva Santos, J.P.T., de Mendonça Cavalcanti, J.C., Botero, W.G., Del Colle, V., 2023. Study of the composition of fractions of manipueira: solid and liquid residues filtered on 0.45 μm membrane and qualitative paper. Rev. Virtual Quím. 15, 1128–1137. https://doi.org/10.21577/1984-6835.20230029.

Menezes, J.B. de C., Catão, H.C.R.M., Costa, C.A. da, Chauca, M.N.C., 2019. Agronomic aspects and quality of minimally processed cassava roots. Agrarian 12, 425–433. https://doi.org/10.30612/agrarian.v12i46.8945.

Moreira, G.F., Peçanha, E.R., Monte, M.B.M., Leal Filho, L.S., Stavale, F., 2017. XPS study on the mechanism of starch-hematite surface chemical complexation. Miner. Eng. 110, 96–103. https://doi.org/10.1016/j.mineng.2017.04.014.

Natarajan, S.R., Krishnamoorthy, R., Alshuniaber, M.A., Gatasheh, M.K., Rajagopal, P., Veeraraghavan, V.P., Palanisamy, C.P., Jayaraman, S., 2025. KDM1A facilitates oncogenic potential in colorectal cancer progression through the activation of AXIN/GSK3β/β-catenin signaling pathways: evidence from integrated transcriptomics and in vitro studies. J. Gene Med. 27 (11). https://doi.org/10.1002/jgm.70053.

Neto, M.d.S.J., Uzeda Antunes Júnior, A., Siqueira Lima, F., Almeida dos Anjos, D., 2015. Potential of Lignocellulosic Fibers for the Production of Second Generation Ethanol.

Ogata, B.H., 2013. University of São Paulo Higher School of Agriculture "Luiz de Queiroz" Characterization of Cellulose, Hemicellulose and Lignin Fractions of Different Sugarcane Genotypes and Potential Use in Biorefineries Piracicaba, 2013 (Thesis). USP, São Paulo.

de Oliveira Schmidt, V.K., de Vasconscelos, G.M.D., Vicente, R., de Souza Carvalho, J., Della-Flora, I.K., Degang, L., de Oliveira, D., de Andrade, C.J., 2023. Cassava wastewater valorization for the production of biosurfactants: surfactin, rhamnolipids, and mannosileritritol lipids. World J. Microbiol. Biotechnol. 39, 65. https://doi.org/10.1007/s11274-022-03510-2.

Padayatchee, S., Ibrahim, H., Friedrich, H.B., Olivier, E.J., Ntola, P., 2025. Solution combustion synthesis for various applications: a review of the mixed-fuel approach. Fluids 10 (4), 82. https://doi.org/10.3390/fluids10040082.

Pandi, N., Sonawane, S.H., Gumfekar, S.P., Kola, A.K., Borse, P.H., Ambade, S.B., Guptha, S., Ashokkumar, M., 2019. Electrochemical performance of starch-polyaniline nanocomposites synthesized by sonochemical process intensification. J. Renew. Mater. 7, 1279–1293. https://doi.org/10.32604/jrm.2019.07609.

Pari, G., Darmawan, S., Prihandoko, B., 2014. Porous carbon spheres from hydrothermal carbonization and KOH activation on cassava and tapioca flour raw material. Procedia Environ. Sci. 20, 342–351. https://doi.org/10.1016/j.proenv.2014.03.043.

Parra, D., Tadini, C., Ponce, P., Lugao, A., 2004. Mechanical properties and water vapor transmission in some blends of cassava starch edible films. Carbohydr. Polym. 58, 475–481. https://doi.org/10.1016/j.carbpol.2004.08.021.

Pei, J., Palanisamy, C.P., Srinivasan, G.P., Panagal, M., Kumar, S.S.D., Mironescu, M., 2024. A comprehensive review on starch-based sustainable edible films loaded with bioactive components for food packaging. Int. J. Biol. Macromol. 274, 133332. https://doi.org/10.1016/j.ijbiomac.2024.133332.

Pei, J., Govindaraj, H., R, S., Kanniappan, G.V., Pandurangan, V., Jayaraman, S., Dhayalan, V.K., Mironescu, M., Mironescu, I.D., Palanisamy, C.P., 2026. Sustainable fabrication of biopolymer-based (starch/PVA) nanoscaffolds loaded with green-synthesized CuO nanoparticles from Sargassum wightii (marine macroalgae): cytocompatibility and antioxidant activity. Biomater. Adv. 182, 214660. https://doi.org/10.1016/j.bioadv.2025.214660.

Ponnusamy, B., Rajagopal, P., Palanisamy, C.P., Veeraraghavan, V.P., Jayaraman, S., 2026. Mechanistic exploration of the anticancer activity of Justicia adhatoda plant leaf ethanolic extract against colon cancer cells: an in silico and in vitro approach. Asian Pac. J. Cancer Prev. 27 (3), 1069–1080. https://doi.org/10.31557/APJCP.2026.27.3.1069.

Prabhakaran, P., Palanisamy, C.P., Shanmugam, A., Damodharan, P., Swaminathan, H., Devaraj, D., Ahalliya, R.M., Velliyur Kanniappan, G., 2025. Isolation, structural characterization, and molecular docking studies on the bioactive compound from n-Hexane extract of *Emilia sonchifolia* (L.) DC against the pancreatic cancer target Aurora 2 Kinase. J. Complement. Integr. Med. 22 (1), 165–172. https://doi.org/10.1515/jcim-2024-0290.

Prasertsilp, P., Pattaragulwanit, K., Kim, B.S., Napathorn, S.C., 2023. Microwave-assisted cassava pulp hydrolysis as food waste biorefinery for biodegradable polyhydroxybutyrate production. Front. Bioeng. Biotechnol. 11. https://doi.org/10.3389/fbioe.2023.1131053.

Primo, J. de O., Borth, K.W., Peron, D.C., Teixeira, V. de C., Galante, D., Bittencourt, C., Anaissi, F.J., 2019. Synthesis of green cool pigments (CoxZn1-xO) for application in NIR radiation reflectance. J. Alloys Compd. 780, 17–24. https://doi.org/10.1016/j.jallcom.2018.11.358.

Primo, J. de O., Bittencourt, C., Acosta, S., Sierra-Castillo, A., Colomer, J.F., Jaerger, S., Teixeira, V.C., Anaissi, F.J., 2020. Synthesis of zinc oxide nanoparticles by ecofriendly routes: adsorbent for copper removal from wastewater. Front. Chem. 8, 1–13. https://doi.org/10.3389/fchem.2020.571790.

de Queiroz, Adriano Melo, de Souza, Luís Gustavo, Souza, Souza, 2020. Quality diagnosis of cassava starch marketed in Rio Branco - AC. Appl. Res. Agrotech. 13, 1–10.

Rebouças, C.S., Freitas, A.G.B. de, Bery, C.C. de S., Silva, I.P. da, Júnior, A.M. de O., Silva, G.F. da, 2015. Use of a system to reduce hydrocyanic acid in the manifold using solar energy. J. Geintec- Manag. Innov. Technol. 5, 1809–1819. https://doi.org/10.47059/GEINTECMAGAZINE.V5I1.488.

Segal, L., Creely, J.J., Martin, A.E., Conrad, C.M., 1959. An empirical method for estimating the degree of crystallinity of native cellulose using the X-ray diffractometer. Text. Res. J. 29 (10), 786–794. https://doi.org/10.1177/004051755902901003.

Shanks, R., Kong, I., 2012. 6 Thermoplastic Starch. China.

Sugumar, P.S., Sivaramakrishnan, R., Velliyur Kanniappan, G., Pandurangan, V., Jayaraman, S., Dhayalan, V.K., Mironescu, M., Mironescu, I.D., Palanisamy, C.P., 2025. Antioxidant and biocompatible CuO-starch/PVA nanoscaffolds via ultrasonic green synthesis using Turbinaria conoides (brown marine macroalgae). Med. Drug Discov. 28, 100238. https://doi.org/10.1016/j.medidd.2025.100238.

Szczepanik, B., Banaś, D., Kubala-Kukuś, A., Szary, K., Słomkiewicz, P., Rędzia, N., Frydel, L., 2020. Surface properties of halloysite-carbon nanocomposites and their application for adsorption of paracetamol. Materials 13, 1–17. https://doi.org/10.3390/ma13245647.

Travalini, A.P., Lamsal, B., Magalhães, W.L.E., Demiate, I.M., 2019. Cassava starch films reinforced with lignocellulose nanofibers from cassava bagasse. Int. J. Biol. Macromol. 139, 1151–1161. https://doi.org/10.1016/j.ijbiomac.2019.08.115.

Varma, A., Mukasyan, A.S., Rogachev, A.S., Manukyan, K.V., 2016. Solution combustion synthesis of nanoscale materials. Chem. Rev. 116, 14493–14586. https://doi.org/10.1021/acs.chemrev.6b00279.

Veiga, J.P.S., Valle, T.L., Feltran, J.C., Bizzo, W.A., 2016. Characterization and productivity of cassava waste and its use as an energy source. Renew. Energy 93, 691–699. https://doi.org/10.1016/J.RENENE.2016.02.078.

Wahyuningtyas, N., Suryanto, H., Rudianto, E., Sukarni, S., Puspitasari, P., 2017. Thermogravimetric and kinetic analysis of cassava starch based bioplastic. J. Mech. Eng. Sci. Technol. 1, 69–77. https://doi.org/10.17977/um016v1i22017p069.

Watcharamongkol, T., Khaopueak, P., Seesuea, C., Wechakorn, K., 2024. Green hydrothermal synthesis of multifunctional carbon dots from cassava pulps for metal sensing, antioxidant, and mercury detoxification in plants. Carbon Resour. Convers. 7, 100206. https://doi.org/10.1016/j.crcon.2023.100206.

Weligama Thuppahige, V.T., Moghaddam, L., Welsh, Z.G., Wang, T., Xiao, H.W., Karim, A., 2023. Extraction and characterisation of starch from cassava (Manihot esculenta) agro-industrial wastes. LWT 182. https://doi.org/10.1016/j.lwt.2023.114787.